Frequency-sheared, time-delayed extreme-ultraviolet pulses produced by high-harmonic generation in argon

W. Kornelis, C. P. Hauri, A. Heinrich, F. W. Helbing, M. P. Anscombe, P. Schlup, J. W. G. Tisch, J. Biegert, and U. Keller

Department of Physics, Institute of Quantum Electronics, ETH Zurich, CH-8093 Zürich, Switzerland

Received January 3, 2005

We report the production of frequency-sheared high harmonics in argon by control of the envelope and chirp of the electric field of the femtosecond driving laser pulse. Using the classic three-step model of high-harmonic generation, we established a direct link between the properties of the harmonics and the fully characterized driving pulses. A simulation of the single-atom response in the strong-field approximation confirms the simple picture and shows good agreement with the experimental results. © 2005 Optical Society of America

OCIS codes: 320.7110, 270.6620.

Extreme ultraviolet (XUV) and soft-x-ray pulses are produced when an intense laser pulse is focused in a gas by high-order harmonic generation.[1,2] For spectroscopic and metrological applications it is desirable to have control over the XUV wavelength and bandwidth as well as to produce two or more XUV pulses in time, with different wavelengths and delays. It is difficult to achieve this control directly in the XUV owing to a lack of suitable optics and techniques. We have chosen to shape the field of the driving laser and to show that, under the right conditions, its structure can be mapped directly to the harmonic field. We present measurements of frequency-sheared harmonic pulses, each of which constitutes two XUV pulses in the time domain, with different photon energy, bandwidth, and intensity. We show that the properties of these frequency-sheared harmonic pulses can be related in a simple way to the electric-field waveform of the generating pulse and that the generating process is dominated by the single-atom response of the medium. For this reason our method does not depend strongly on the target and focusing conditions used and should thus be applicable to the whole energy range reached by high-harmonic generation (HHG). Further, this technique can be extended to more than two XUV pulses. Such pulses could be used, for example, for single-shot, time-resolved probing of high-density laser plasmas[3]; a number of delay points could be sampled in one shot by use of a spectrometer to separate the XUV pulses on a time-integrated detector array. Time-separated and frequency-sheared pulses are also a prerequisite for any achievement of spectral interferometry for direct electric-field reconstruction (SPIDER) in the XUV range.[4,5] Our method can potentially give access to this pulse characterization method because it produces the required pulses in a simple manner in the interaction volume. The process of HHG is commonly divided into two parts: the single-atom response, which is the interaction of an atom with the electric field of the laser pulse and is theoretically described by the semiclassical three-step model,[6,7] and the propagation of the laser and harmonic fields in the medium governed by Maxwell's equations, which describe the phase matching of all the single atomic emitters in the medium, influenced in a nontrivial way by macroscopic properties of the driving laser and gas medium.[8] We used a standard chirped-pulse amplification laser system to produce 35 fs pulses (center wavelength, 795 nm), with an energy of as much as 1 mJ and at a repetition rate of 1 kHz. Our amplifier system[9] was equipped with an acousto-optic programmable dispersive filter (FastLite, Dazzler),[10] which allowed us to control the spectral phase and thus also the temporal properties of the amplified pulses. We generated high harmonics by focusing the pulses into a 14 cm long capillary[11] with an inner diameter of 0.26 mm and a pressure distribution from 0.32×10^5 Pa argon at the entry of the capillary to vacuum (10^{-2} Pa) at its exit. The peak intensity in the interaction region was approximately 1×10^{14} W/cm^2, and harmonic orders of 17 to a cutoff at 23 were measured with a resolution of 0.05 nm in this range by an XUV spectrometer (McPherson 248/310G; 600 line/mm grating) fitted with a microchannel plate detector.

To investigate the dependence of the high harmonics on the properties of the driving electric field, we used the Dazzler filter to shape the input electric field, which was characterized by a real-time infrared SPIDER setup,[12,13] while we simultaneously recorded the harmonic spectrum. Using the Dazzler, we changed the third-order dispersion component of the spectral phase of an initially linearly chirped pulse to produce chirped driving pulses with double-peaked temporal pulse envelopes. Producing the two time-delayed pulses in this way prevented geometrical separation and other difficulties typically associated with interferometric setups.

The SPIDER measurements allowed a full reconstruction to be made of the electric field in time and in frequency. The Wigner function[14] allows one to visualize the full time–frequency structure of an ultrashort pulse. It describes the temporal evolution of

0146-9592/05/131731-3/$15.00

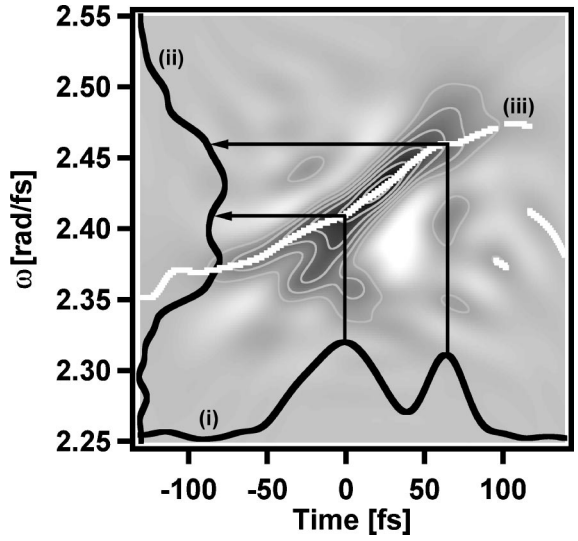

Fig. 1. Density plot of the Wigner distribution of a driving pulse, in which the solid curves show (i) the temporal pulse, (ii) the spectrum, and (iii) the instantaneous frequency.

the frequency components that compose the pulse. In Fig. 1 a density plot of the Wigner function for a driving pulse is shown. The integral over frequency of the Wigner function gives the temporal pulse shape [curve (i)], and similarly the time integral results in the spectrum [curve (ii)]. Of particular relevance is the instantaneous frequency at a given time, which one may obtain by finding the frequency of the maximum of the Wigner distribution at that time[15] [curve (iii)].

In Fig. 2 the measured harmonic spectra are shown for five driving pulses, labeled (a)–(e), that we formed by adding (a) 0, (b) 1500, (c) 4000, (d) 8000, and (e) 10,000 fs^3/rad of third-order dispersion to the spectral phase of the laser pulse.

Apart from spectra (a) and (e), each of which contains only a single peak at each harmonic order, in the other spectra each of the harmonics is split into two separate peaks. The lower-energy peak is found to have a higher intensity and a small bandwidth, whereas the peak shifted to higher energies has a lower intensity and a larger bandwidth.

The driving pulse shown in Fig. 1 generated the harmonic spectrum (c) in Fig. 2. It consisted of two subpulses, separated by 60 fs. The first subpulse was 60 fs in duration and had a higher peak intensity than the second subpulse, which was 30 fs long. The tilt of the Wigner function indicates that a chirp was present; from the distribution it can be established that the first subpulse contained predominantly the low-frequency part of the pulse spectrum whereas the second subpulse contained the high-frequency part (arrows in Fig. 1) The pulse characterization provides the explanation that the first subpulse generated a high-intensity, low-bandwidth, low-photon-energy peak for each harmonic order; the second subpulse, the low-intensity, high-bandwidth, and high-photon-energy peak. Because of the nonlinear nature of HHG (the harmonic intensity scales typically as the >5th power of the laser intensity) one can assume that the harmonics are generated predominantly near the pulse peaks and therefore that only frequency components that occur near the peaks contribute significantly to the generation of the harmonics. The frequency components near the pulse peaks of the two subpulses are spectrally separated because of the chirp, and one thus expects a double-peaked harmonic structure. Moreover, the first subpulse is longer, so more cycles contribute to the harmonic, leading to a harmonic peak with a smaller bandwidth. Finally, the higher peak intensity of the first subpulse leads to an increased harmonic yield, and the resultant harmonic peak is higher than that generated by the second subpulse.

The fraction of argon atoms ionized by the first 60 fs long pulse (peak intensity, 1×10^{14} W/cm^2) was estimated according to Ammosov–Delone–Krainov theory[16] to be less than 1%. Importantly, the negligible degree of ionization depletion of the generating medium and low free-electron phase mismatch allowed us to treat the second pulse independently from the first. We can explain the remaining spectra of Fig. 2 in the same way by analyzing the properties of the respective driving electric fields (not shown).

For a more rigorous analysis of the picture presented above, we carried out a numerical simulation of the single-atom response in the strong-field approximation,[6,7] using as input the measured electric field of the pulse shown in Fig. 1. Because of the larger divergence of the harmonic radiation stemming from the long electron trajectories,[7] our narrow-angle spectrometer measured predominantly the contribution of the short trajectories. We therefore

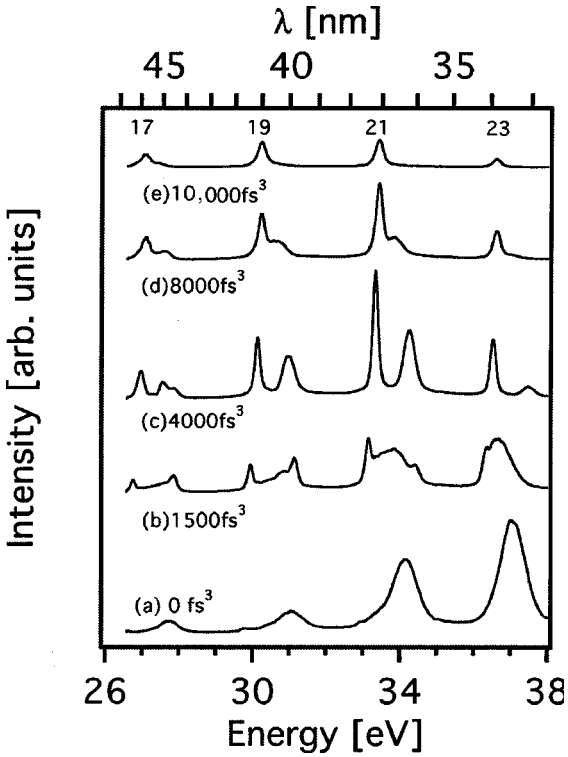

Fig. 2. Measured harmonic spectra for orders 17–23, with third-order dispersion of the driving pulses increasing from bottom to top (see text). Each curve is on the same intensity scale but shifted vertically for clarity.

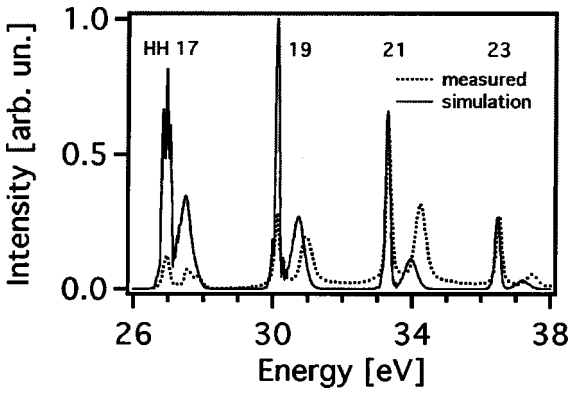

Fig. 3. Simulated and measured harmonic spectra for curve (c) of Fig. 2.

suppressed the contribution of the long trajectories in the simulation by restricting the time integration to the maximum electron recollision time in the short trajectory.

The result of our simulation for curve (c) in Fig. 2 is shown in Fig. 3 (solid curve). The simulated spectrum was normalized to the measured intensity of the 23rd harmonic and reproduces all the features of the measured data (dashed curve), i.e., for each harmonic order two peaks are present, a higher-intensity peak with lower bandwidth and at lower photon energy and a lower-intensity peak with larger bandwidth and at higher photon energy. The simulation does not include phase-matching effects, so the measured relative peak intensities of the different harmonic orders are not accurately reproduced. However, for the substructure of each harmonic order a relatively good agreement between the measured spectra and the numerical simulation was found, indicating an effect dominated by the single-atom response: the frequency positions of the qth-harmonic double-peak structure are simply given by q times the instantaneous frequency at the peaks of the driving laser subpulses.[17]

In conclusion, we have demonstrated a flexible technique based on high-harmonic generation in the weakly ionized regime for the production of frequency-sheared, time-delayed XUV pulses through shaping of a single femtosecond laser pulse. A numerical calculation of the single-atom response in the strong-field approximation with the measured driving electric field as input resulted in good agreement with the measured harmonic spectrum. Frequency-sheared, time-delayed XUV pulses with controllable energy and bandwidth that are synchronized precisely with the driving laser pulse may find application in a number of pump–probe applications, such as femtosecond probing of laser plasmas and, with a smaller frequency shear than presented in this Letter, are a prerequisite for the XUV implementation of SPIDER.[4,5] The small degree of ionization observed with our technique does not alter phase matching significantly, in contrast to other multipulse HHG setups in which spatially separated high-harmonic beams are used. Note that the broader bandwidths associated with shorter laser pulses than used here (down to the few-cycle limit) offer even greater control over the time-frequency structure of the XUV radiation.

J. Tisch's present address is Department of Physics, Imperial College, London, UK. This research was supported by the Swiss National Science Foundation (QP-NCCR) and by ETH Zürich. We acknowledge the support of European Union FP6 program "Structuring the European Research Area" and the Marie Curie Research Training Network XTRA (contract FP6-505138). J. Biegert's e-mail address is biegert@phys.ethz.ch.

References

1. A. McPherson, G. Gibson, H. Jara, U. Johann, T. S. Luk, I. A. McIntyre, K. Boyer, and C. K. Rhodes, J. Opt. Soc. Am. B **4**, 595 (1987).
2. M. Ferray, A. L'Huillier, X. F. Li, L. A. Lompré, G. Mainfray, and C. Manus, J. Phys. B **21**, L31 (1988).
3. W. Theobald, R. Hässner, C. Wülker, and R. Sauerbrey, Phys. Rev. Lett. **77**, 298 (1996).
4. F. Quéré, J. Itatani, G. L. Yudin, and P. B. Corkum, Phys. Rev. Lett. **90**, 073902 (2003).
5. E. Cormier, I. A. Walmsley, E. M. Kosik, A. S. Wyatt, L. Corner, and L. F. DiMauro, Phys. Rev. Lett. **94**, 033905 (2005).
6. P. B. Corkum, Phys. Rev. Lett. **71**, 1994 (1993).
7. M. Lewenstein, Ph. Balcou, M. Yu. Ivanov, A. L'Huillier, and P. Corkum, Phys. Rev. A **49**, 2117 (1994).
8. P. Antoine, A. L'Huillier, and M. Lewenstein, Phys. Rev. Lett. **77**, 1234 (1996).
9. W. Kornelis, M. Bruck, F. W. Helbing, C. P. Hauri, A. Heinrich, J. Biegert, and U. Keller, Appl. Phys. B **79**, 1033 (2004).
10. F. Verluise, V. Laude, J.-P. Huignard, P. Tournois, and A. Migus, J. Opt. Soc. Am. B **17**, 138 (2000).
11. A. Rundquist, C. G. Durfee III, Z. Chang, C. Herne, S. Backus, M. M. Murnane, and H. C. Kapteyn, Science **280**, 1412 (1998).
12. L. Gallmann, D. H. Sutter, N. Matuschek, G. Steinmeyer, U. Keller, C. Iaconis, and I. A. Walmsley, Opt. Lett. **24**, 1314 (1999).
13. W. Kornelis, J. Biegert, J. W. G. Tisch, M. Nisoli, G. Sansone, C. Vozzi, S. De Silvestri, and U. Keller, Opt. Lett. **28**, 281 (2003).
14. J. Paye, IEEE J. Quantum Electron. **28**, 2262 (1992).
15. K.-H. Hong, J.-H. Kim, Y. H. Kang, and C. H. Nam, Appl. Phys. B: Lasers Opt. **74**, S231 (2001).
16. F. A. Ilkov, J. E. Decker, and S. L. Chin, J. Phys. B **25**, 4005 (1992).
17. J. Mauritsson, P. Johnsson, R. Lopez-Martens, K. Varju, W. Kornelis, J. Biegert, U. Keller, M. B. Gaarde, K. J. Schafer, and A. L'Huillier, Phys. Rev. A **70**, 21801 (2004).